

# Gapless spin liquid in the kagome Heisenberg antiferromagnet with Dzyaloshinskii-Moriya interactions

Chih-Yuan Lee,<sup>1</sup> B. Normand,<sup>2</sup> and Ying-Jer Kao<sup>1,3,4</sup>

<sup>1</sup>*Department of Physics, National Taiwan University, Taipei 10617, Taiwan*

<sup>2</sup>*Neutrons and Muons Research Division, Paul Scherrer Institute, CH-5232 Villigen PSI, Switzerland*

<sup>3</sup>*National Center of Theoretical Sciences, National Tsing Hua University, Hsinchu 30013, Taiwan*

<sup>4</sup>*Department of Physics, Boston University, Boston, MA 02215, USA*

(Dated: December 4, 2018)

A preponderance of evidence suggests that the ground state of the nearest-neighbor  $S = 1/2$  antiferromagnetic Heisenberg model on the kagome lattice is a gapless spin liquid. Many candidate materials for the realization of this model possess in addition a Dzyaloshinskii-Moriya (DM) interaction. We study this system by tensor-network methods and deduce that a weak but finite DM interaction is required to destabilize the gapless spin-liquid state. The critical magnitude,  $D_c/J \simeq 0.012(2)$ , lies well below the DM strength proposed in the kagome material herbertsmithite, indicating a need to reassess the apparent spin-liquid behavior reported in this system.

## I. INTRODUCTION

Quantum spin liquids have become a central focus of efforts in condensed matter physics to understand phenomena including quantum entanglement, high-dimensional fractionalization, and topological properties in many-body systems [1]. In this context, the  $S = 1/2$  kagome Heisenberg antiferromagnet (KHAF) is one of the most fundamental and controversial models to have been studied both theoretically and experimentally [2]. On the theoretical and numerical side, extensive and highly refined analyses by a wide range of methods have come out in favor of both a gapped [3–11] and a gapless [12–19] spin-liquid ground state. However, with the most recent studies by both tensor-network [17, 18] and density-matrix renormalization-group (DMRG) [19] methods indicating a gapless  $U(1)$  spin liquid, evidence is mounting that the physics of the KHAF may be driven by maximizing the kinetic energy of gapless Dirac spinons [12, 13, 18].

Experimental approaches to the kagome problem have focused largely on the material  $\text{ZnCu}_3(\text{OH})_6\text{Cl}_2$  (herbertsmithite) [20], which offers an ideal kagome lattice of  $S = 1/2$   $\text{Cu}^{2+}$  ions. No evidence has been found for long-ranged magnetic order, spin freezing, or indeed a spin gap at temperatures as low as 50 mK [21–24], which is 3000 times smaller than the characteristic exchange energy,  $J$ . However, some neutron spectroscopy and nuclear magnetic resonance data have been interpreted more recently as showing a small gap [25, 26]. While extensive studies have been devoted to the characterization of impurities in herbertsmithite [27–30], it is important not to lose sight of the possibility that the physics of the system could be influenced by its Dzyaloshinskii-Moriya (DM) interactions. DM terms appear naturally in a spin Hamiltonian as a consequence of spin-orbit interactions, and cancel only when the bond is a center of inversion symmetry. Thus they are ubiquitous in low-symmetry Cu materials, where the square geometry of the active  $d_{x^2-y^2}$  orbital does not fit the structural geometry, as is

the case for the triangular motifs of the kagome lattice. An early determination of the DM interaction in herbertsmithite by electron spin resonance (ESR) [31] proposed the values  $D_z = 0.08J$  for the out-of-plane component and  $D_\rho = 0.01J$  in-plane, while a subsequent theoretical analysis of the same data suggested the bounds  $0.044 \leq D_z/J \leq 0.08$  [32].

Previous studies of DM interactions in the KHAF were based on exact diagonalization (ED) of small clusters. Shortly after the discovery of herbertsmithite, efforts were made [33, 34] to interpret powder susceptibility measurements at intermediate and higher temperatures on the basis of linked-cluster expansions and ED calculations using clusters of 12 and 15 sites. While both in- and out-of-plane DM components were considered, few definite conclusions were possible due to uncertainty over the impurity contributions to the experimentally measured quantities. ED studies of the ground state were performed both by considering the pure system on clusters of up to 36 sites [35] and by considering the model in the presence of a single impurity on clusters of up to 26 sites [36]; partly out of numerical convenience, these calculations were performed using only an out-of-plane DM term. ED is known to predict a gapped ( $Z_2$ ) spin-liquid ground state, although the magnitude of this gap has never been agreed upon [37] and the result is now suspected to be an artifact of the small cluster size [38]. This gapped state is naturally robust against small  $D_z$ , and a transition to the  $120^\circ$  magnetic order favored by the out-of-plane DM term was found at  $D_c \simeq 0.10J$  [35, 36]. Schwinger-boson methods, which also favor a gapped ground state, have been used [39, 40] to obtain similar  $D_c$  values, subject to uncertainties over representative values of  $S$  and  $N$  [for  $SU(N)$  spins] to employ in this framework. Although the same methods have also been used to suggest that  $D_z$  may induce a chiral state [41], DMRG studies [42] find only proximity to the chiral spin liquid. This latter analysis obtained  $D_c = 0.08J$  while interpreting the ground state at  $D < D_c$  as a gapless spin liquid. A recent functional renormalization-

group (FRG) analysis [43], which also was later shown to suggest that the ground state of the KHAF is a gapless  $Z_2$  spin liquid [44], has again obtained a similar result,  $D_c = 0.12(2)J$ .

In contrast to these earlier studies, we employ a numerical technique, specifically a tensor-network ansatz based on projected entangled simplex states (PESS), known to provide a gapless spin-liquid ground state when  $D = 0$ . We will show that, despite its lack of a “protective” gap, or even a known protective topology, the  $U(1)$  spin liquid persists to small but finite values of the out-of-plane DM interaction.

The structure of this manuscript is as follows. In Sec. II we introduce the model and summarize the tensor-network methods we use to analyze it, focusing on the technical developments we have introduced in the present calculations. In Sec. III we discuss the Husimi lattice, for which extremely accurate PESS calculations are possible, to fulfil the dual roles of benchmarking the extrapolation of our numerical data and of benchmarking the physics of our kagome results. In Sec. IV we present the energy and magnetization of the kagome lattice for different values of the DM anisotropy. We use the Husimi benchmark in Sec. V to deduce the critical DM coupling strength for the suppression of spin-liquid behavior and close in Sec. VI by commenting on the theoretical aspects and experimental context of our findings.

## II. MODEL AND METHODS

To investigate the effects of DM interactions in the KHAF, we consider the model

$$H = \sum_{\langle ij \rangle} J \vec{S}_i \cdot \vec{S}_j + D_z \hat{z} \cdot (\vec{S}_i \times \vec{S}_j). \quad (1)$$

For consistency with previous studies [35, 36, 43], and also motivated by the ESR analysis [31], we consider only an out-of-plane DM component,  $D_z$  (henceforth  $D$ ). Following the results of Ref. [18], that the gapless spin-liquid regime exists over only a narrow range of next-neighbor coupling, we do not consider any further-neighbor Heisenberg terms. Following the logic expressed in Ref. [31] on the basis of the  $g$ -factor, that anisotropies in the exchange interaction are smaller than DM terms by an order of magnitude [in  $(g - 2)/g$ , which is approximately 0.1 in herbertsmithite], we do not consider any XXZ character in Eq. (1). However, we comment that exchange anisotropies have been estimated from ESR data in the candidate kagome material vesignieite [45].

Numerical methods based on tensor-network representations of the quantum many-body wave function [46–48] have matured only recently to the point at which they can be relied on for the quantitative analysis of problems at the leading edge of research in strongly correlated systems [49, 50]. As generalized matrix-product states, tensor-network wave functions obey the area law of en-

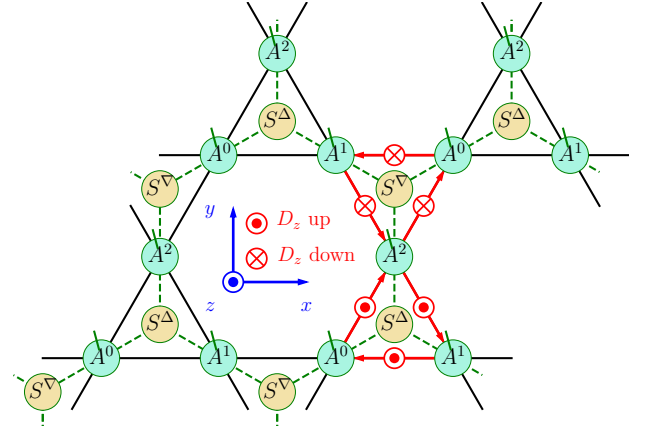


FIG. 1. Graphical representation of the kagome lattice, the geometry of the DM interactions in Eq. (1), and the 3-PESS ansatz.  $S^\Delta$  and  $S^\nabla$  are the simplex tensors, which encode the multipartite entanglement of the kagome triangles, and  $A^0$ ,  $A^1$ ,  $A^2$  are projection tensors.

tanglement [51]. Of key importance in the kagome problem, their structure allows a real-space renormalization-group approach by which one may access the limit of infinite lattice size. In overall structure, our calculations follow the approach of Refs. [52] and [18], summarized in the remainder of this section, but differ in a number of details and are performed using code we have written based on the Uni10 tensor-network library (<https://uni10.gitlab.io/>) [53].

### A. PESS as a wave-function ansatz

The crucial element of PESS [52], which goes beyond the conventional pairwise projected entangled pair states (PEPS) construction [50], is its ability to capture the nontrivial multipartite entanglement within each lattice unit, or simplex [52, 54, 55], of a frustrated quantum spin system. By the geometry of the kagome lattice, and of the nearest-neighbor interactions (denoted  $\langle ij \rangle$ ) in Eq. (1), the system is described naturally by the “3-PESS” shown in Fig. 1, where  $S^\Delta$  and  $S^\nabla$  are the two types of three-site simplex tensor and  $A^0$ ,  $A^1$ , and  $A^2$  are projection tensors. The dangling solid lines in Fig. 1 denote the physical (spin) degrees of freedom, which add a physical tensor dimension  $d = 2$  for  $S = 1/2$ . The inter-tensor bonds are virtual objects whose tensor bond dimension, which here we denote by  $\chi$ , sets the maximal number of virtual states that can be kept within the ansatz and functions as the truncation parameter in the tensor-network representation. We impose translational symmetry and hence Fig. 1 corresponds to the mathematical expression of the wave function

$$|\Psi\rangle = \text{Tr}(\dots S_{a'b'c'}^\alpha A_{a'a,\sigma_i}^0 A_{b'b,\sigma_j}^1 A_{c'c,\sigma_k}^2 \dots) |\dots \sigma_i \sigma_j \sigma_k \dots\rangle,$$

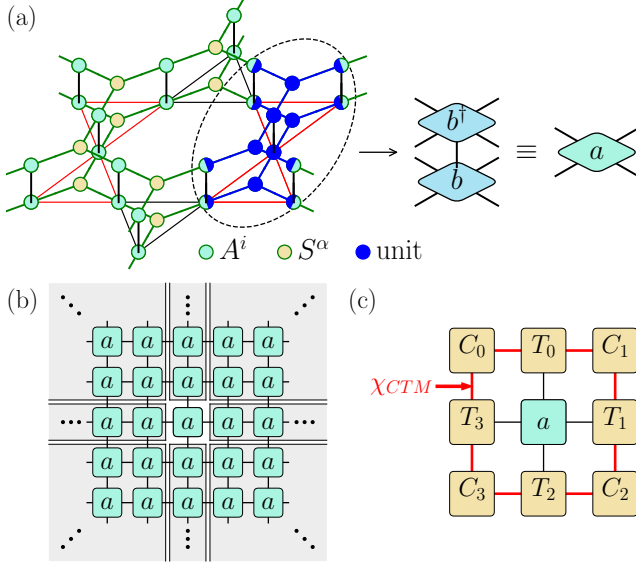


FIG. 2. (a) Representation of a bilayer of 2D infinite tensor networks, whose repeat units may be combined into a single tensor,  $a$ , and whose contraction is required in the calculation of a physical expectation value. (b) Illustration of the square lattice of  $a$  tensors and the blocking scheme adopted in the CTM approach. (c) Approximation to the environment of a single  $a$  tensor on the square lattice by four  $C$  and four  $T$  tensors, each with boundary bond dimension  $\chi_{CTM}$ .

where  $\alpha = \Delta, \nabla$  denote two simplex tensors for up- and down-triangles of the lattice,  $\{\sigma_i, \sigma_j, \dots\}$  denote the spin basis states on lattice sites  $i, j, \dots$ , and  $\{a, b, \dots\}$  denote the  $\chi$  virtual bond states.

A PEPS/PESS representation is manipulated efficiently by an imaginary-time projection technique [56] similar to the infinite time-evolving block-decimation method [57, 58], which we apply to project out the ground-state wave function. By decomposing Eq. (1) into  $H = H_\Delta + H_\nabla$ , where the two terms contain respectively all Hamiltonian terms on up- and down-pointing triangles, we approach the optimized PESS ground state by applying  $e^{-\tau H_\Delta}$  and  $e^{-\tau H_\nabla}$  successively on a random initial wave function, where  $\tau$  is a small imaginary time step. We comment that this procedure breaks the threefold symmetry of the kagome system, with the result that evaluations of the two-triangle unit are actually performed on the square lattice, as depicted schematically in Fig. 2(a). We verify the restoration of threefold symmetry in the limit of small  $\tau$  and large  $\chi$  during our calculations of physical expectation values [52].

The projection operators  $e^{-\tau H_\alpha}$  act on the full triangular simplex (schematically  $S^\alpha A^0 A^1 A^2$ ) to produce a contracted tensor with dimension  $(d\chi)^3$  at each step. For the truncation of this tensor, we work exclusively at the level of the simple-update method [49, 56, 59], based on local tensor contractions and explained in detail for the kagome lattice in Ref. [52]; this approach has been found to yield the optimal PESS ground states based

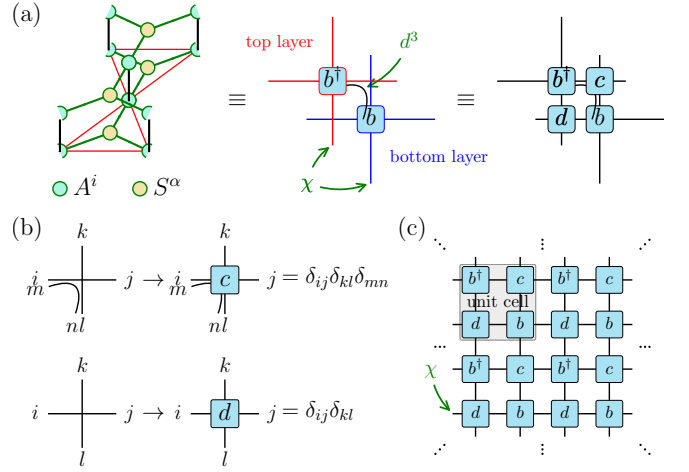


FIG. 3. Representation of the dimension-reduction procedure. (a) The calculation of an expectation value is the contraction of two tensor networks whose minimal unit is  $b^\dagger$  in the top layer and  $b$  in the bottom layer, the two being connected by contraction of the physical bond. To adopt the one-layer CTM method, we introduce additional contraction tensors,  $c$  and  $d$ . (b) Pictorial definition of the tensors  $c$  and  $d$ . (c) Resulting reduction of the tensor network in Fig. 2(b), which has bond dimension  $\chi^2$  and one-tensor unit cell, to a network with bond dimension  $\chi$  and four-tensor unit cell.

on efficiency of convergence and accessible  $\chi$  values. We comment that the simple-update treatment is essentially complete on the Husimi lattice [55], where the simplex tensors have no connection other than their local bonds, and we will exploit this property in Sec. III to assist in interpreting our kagome calculations.

## B. Computing expectation values by CTM

The PESS wave function we obtain is an infinite two-dimensional (2D) tensor network. For the calculation of physical expectation values,  $\langle \Psi | Q | \Psi \rangle$ , it is necessary to contract this network, or more specifically its “square,” represented in Fig. 2(a). A number of approaches exist for this procedure, specifically the use of boundary matrix-product states (bMPS) [57, 58], which are used to perform successive 1D contractions [18, 52], of corner-transfer-matrix (CTM) methods [60, 61], which proceed directly in 2D, and the hybrid method of channel environments [62]. Here we have adopted the CTM scheme, in which the original problem based on tensors  $a$  [Fig. 2(b)] is approximated by  $C$  and  $T$  tensors as shown in Fig. 2(c), and the accuracy of the approximated environment is controlled by the boundary bond dimension,  $\chi_{CTM}$ . The  $C$  and  $T$  tensors are deduced from  $a$  and from isometry operations [63–65] by constructing an iterative renormalization scheme based on the invariance of the system under the addition of rows and columns. Technically, it is necessary to store the environments for all tensors within

the unit cell during the iteration.

To maximize the  $\chi$  value for which we can compute physical quantities, we follow a recent proposal [66] for optimizing the tensor contraction process. This method, originally proposed to optimize bMPS contractions and employed in Ref. [18] to extend the maximum  $\chi$  attainable on the kagome lattice from 15 to 25, can also be applied within a CTM approach. Its essence is to transform the original calculation, which is the contraction of a double-layer tensor network with bond dimension  $\chi^2$  and a one-tensor unit cell [Fig. 3(a)], to the contraction of a single-layer network with a  $2 \times 2$  unit cell, as represented in Fig. 3(c). The upper ( $b^\dagger$ ) and lower ( $b$ ) tensor networks are combined by introducing the tensors [Fig. 3(b)]

$$c_{ijklmn} = \delta_{ij}\delta_{kl}\delta_{mn},$$

$$d_{ijkl} = \delta_{ij}\delta_{kl}.$$

Because CTM is an approximate contraction method, in which the error is controlled by  $\chi_{CTM}$ , the variational principle is not applicable and any physical expectation value may increase or decrease with increasing  $\chi_{CTM}$ . The expectation values on which we focus here are the ground-state energy per site,  $E = \frac{1}{6}(E_\Delta + E_\nabla)$ , and the staggered magnetization (ordered moment per site),

$$M = \frac{1}{3} \sum_{i=1,2,3} \sqrt{\langle S_i^x \rangle^2 + \langle S_i^y \rangle^2 + \langle S_i^z \rangle^2}, \quad (2)$$

where  $i$  denotes the three sites of an up- or down-simplex in the translationally invariant infinite system, and as noted above all three sites and the two simplex types become equivalent in the limits of small  $\tau$  and large  $\chi$  and  $\chi_{CTM}$ . To analyze convergence as a function of  $\chi_{CTM}$ , in Fig. 4 we show the evolution of  $E$  and  $M$  of the KHAF for a representative DM interaction  $D = 0.016$  and for  $\chi$  values of 20 and 25. We observe that both  $E$  and  $M$  show well-controlled convergence with increasing  $\chi_{CTM}$  and that, beyond the value  $\chi_{CTM} \approx \chi^2$ , where the errors due to the finite value of  $\chi_{CTM}$  are expected to be small compared with those due to the finite  $\chi$ , the relative changes in both quantities are extremely small.

### III. HUSIMI HAF WITH DM INTERACTIONS

The nature of our PESS results is that we obtain physical expectation values, specifically  $E$  and  $M$  of the preceding section, for a series of finite values of the truncation parameter, which is the tensor bond dimension,  $\chi$ . The physics of the true ground state at any given value of  $D$  is obtained by extrapolating this series to the limit of infinite  $\chi$ . To illustrate the nature of this extrapolation in the most systematic way possible, we turn to the Heisenberg antiferromagnet, with DM interactions, on the Husimi lattice.

The Husimi lattice, whose geometry we show in the inset of Fig. 6, is a Bethe lattice of corner-sharing triangles. It possesses the same local coupled-triangle physics

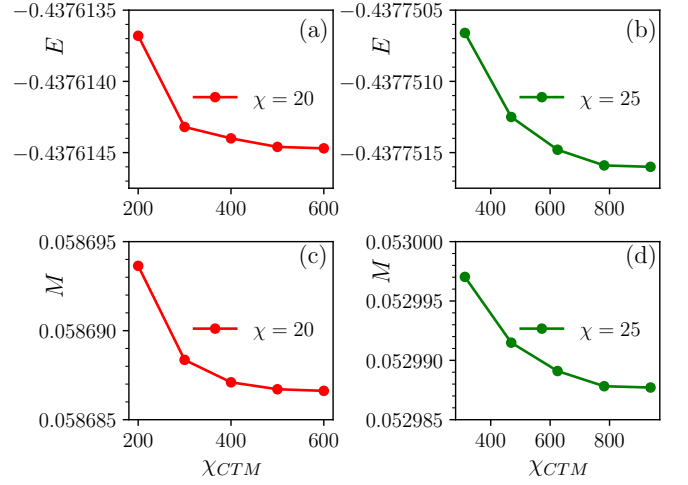


FIG. 4. Convergence of the ground-state energy,  $E$  (a,c), and staggered magnetization,  $M$  (b,d), as functions of the boundary bond dimension,  $\chi_{CTM}$ , for bond dimensions  $\chi = 20$  (a,b) and 25 (c,d).

as the kagome lattice, but all longer paths that connect spins in the KHAF are entirely absent. We consider only the infinite Husimi lattice, which possesses translational invariance and is distinct from the “Husimi tree,” a finite system in which half of the sites are located on the boundary, leading to some singular properties [55].

Physically one may anticipate that the Husimi HAF is a “less frustrated” quantum spin model than the KHAF, giving a lower tendency to spin-liquid formation. From the viewpoint of PESS calculations, the absence of all longer loops means that the simple-update method is effectively complete for the Husimi lattice [55], in the sense that no additional measures are required to account for longer paths, for example in the calculation of bond environment terms [52]. As a result, the problem remains at the level of a local minimization, making it possible to reach very large values of  $\chi$  and hence to perform very reliable extrapolation of all physical expectation values to the large- $\chi$  limit.

We focus for illustration on  $M(\chi)$  in the Husimi HAF, which we show in Fig. 5 for three different values of  $D$ . We stress that  $M$  is always finite in PESS calculations on the Husimi and kagome lattices at finite values of  $\chi$  [18], and that only reliable extrapolation to infinite  $\chi$  can be used to determine whether or not the magnetic order is real; however, a real  $120^\circ$ -ordered antiferromagnetic phase is expected on both lattices at larger values of  $D$  [35, 36]. Guided by the possibility of gapless spin-liquid or antiferromagnetic phases at infinite  $\chi$ , we consider only power-law fitting forms. With many data points available up to  $\chi = 280$ , we obtain reliable fits and accurate intercepts. When  $D = 0$ , we obtain an accurate fit to  $M \propto \chi^{-a}$ , i.e. we find in accord with Ref. [55] that  $M = 0$  in the limit of infinite  $\chi$  and that the exponent is  $a = 0.583(5)$ . For all finite values of  $D$ , we find that  $M(\chi \rightarrow \infty)$  is finite, meaning that the gapless spin-liquid

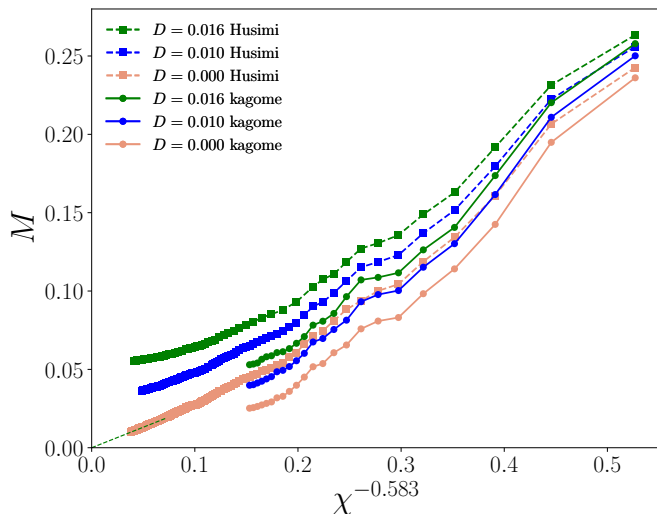


FIG. 5. Extrapolated  $M$  as a function of  $\chi$  for the Husimi and kagome systems at three different values of the DM interaction.

phase is present in the Husimi HAF only at  $D = 0$ .

To consider the evolution of the physical properties of the system with  $D$ , and with a view to examining the nature of a possible quantum phase transition on the kagome lattice from an ordered antiferromagnetic phase at higher  $D$  to a quantum spin liquid [35, 36], we illustrate the situation for the Husimi lattice. Because it is not clear that data points at high  $D$  should fall in the quantum critical regime, we adopt a windowing procedure where we fit different numbers of data points (starting at point  $(0, 0)$ , to which we ascribe zero error bar [55]) and take the fit with the lowest reduced chi-squared value as our best estimate. As shown in Fig. 6, we deduce that  $M = cD^b$  with  $b = 1.10(2)$ , implying a nearly, but not exactly, linear relation between the ordered moment and the DM interaction away from the critical (gapless) phase at  $D = 0$ .

In summary, the Husimi HAF provides crucial qualitative and quantitative benchmarks for our PESS calculations, showing that magnetically ordered states have the lowest energies for spatially infinite systems at finite  $\chi$ , and that  $E(\chi)$  and  $M(\chi)$  are algebraic. The vanishing of  $M(\infty)$  at  $D = 0$  presents a reliable example of a gapless spin liquid, and the finite  $M(\infty)$  at all finite  $D$  may be expected from the somewhat pathological Bethe-lattice geometry [18]. We caution that the functional forms we deduce from our Husimi data do not apply at small  $\chi$  (Fig. 5) and that by this measure all of our kagome results are in the small- $\chi$  regime, which will determine our treatment of the kagome data in Sec. V.

#### IV. KHAF ENERGY AND MAGNETIZATION

Turning now to the KHAF, it was shown in Ref. [18] that simple-update PESS calculations up to  $\chi = 25$  yield

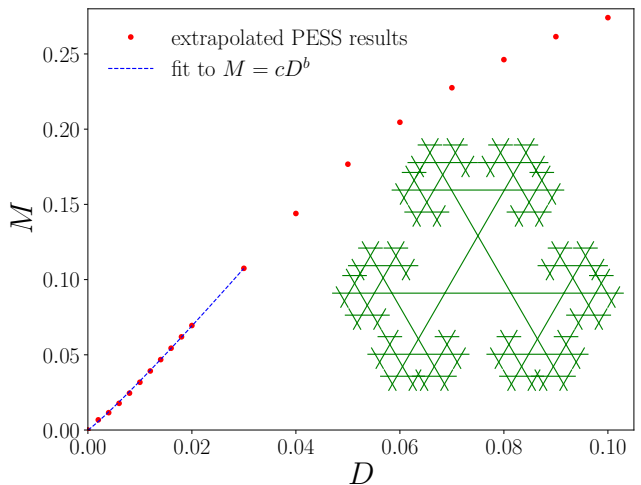


FIG. 6.  $M$  as a function of  $D$  on the Husimi lattice, showing a near-linear scaling with proportionality constant  $c = 5.2(2)$  and exponent  $b = 1.10(2)$ . Inset: Husimi lattice.

a ground-state energy for the nearest-neighbor model,  $E(\chi \rightarrow \infty)$ , that lies below the values obtained from all other techniques (apart from DMRG calculations for certain cylindrical geometries).  $E(\chi)$  was found to obey an algebraic convergence with  $\chi$ , as on the Husimi lattice [55], indicating a gapless ground state [67]. Also as on the Husimi lattice, the PESS wave function was found to have a finite  $120^\circ$  magnetic order at all finite  $\chi$  values, but with the algebraic  $M(\chi)$  lying well below the analogous Husimi value.

In Fig. 7 we extend these results to include DM interactions. It is clear that finite  $D$  values push down the ground-state energy in a monotonic manner [Fig. 7(a)], implying a relief of the kagome frustration. Equally clear is that  $M(\chi)$  is pushed upwards by the effect of  $D$ , in the same monotonic manner, implying that that trend is towards a magnetic state, as already found in the Husimi case. Although the  $120^\circ$  state on each triangle remains frustrated both for the Heisenberg term and for the DM term, it appears that this frustration is lower than that inherent in the gapless spin liquid. However, our kagome results terminate at  $\chi = 25$ , a bond dimension reachable only at great computational cost. As implied in Sec. III, and made clear by Fig. 5, the data continue to show artifacts at these  $\chi$  values that prevent a reliable extrapolation.

#### V. PHASE DIAGRAM

To make progress under these circumstances in understanding the physics of the KHAF, we continue to exploit the comparison with the Husimi system. In Ref. [18] the stability of the gapless spin-liquid phase was investigated by adding a next-neighbor coupling,  $J_2$ , to the KHAF, and stability was demonstrated over a finite, if narrow,



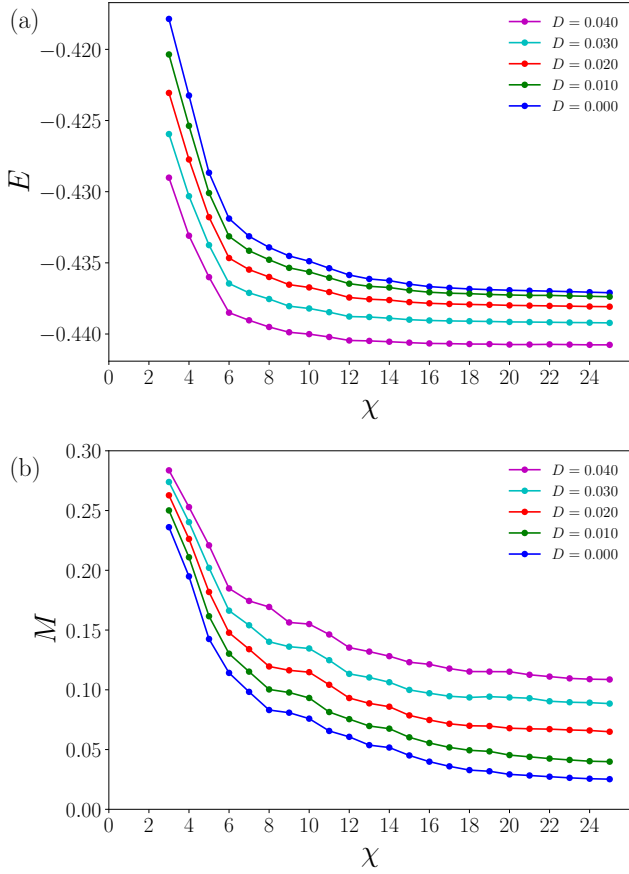


FIG. 7. KHAF with DM interactions. (a)  $E$  as a function of  $\chi$ , shown for three different values of  $D$ . (b)  $M$  as a function of  $\chi$ , shown for three different values of  $D$ .

regime of  $J_2$  by comparing both  $E$  and  $M$ . Here we adopt an analogous procedure to investigate the effect of  $D$  on the gapless spin liquid by comparing our magnetization results.

In Fig. 8(a) we compare the magnetization of the KHAF,  $M(\chi)$ , computed for several values of  $D$ , with  $M(\chi)$  for the Husimi HAF at  $D = 0$ . Because the Husimi system marks the upper limit of spin-liquid behavior, we assert that all magnetization curves lying below this one correspond to the parameter regime in which the KHAF has a spin-liquid ground state. By its algebraic nature, this spin liquid will be gapless for all  $D$  values below the critical one where order sets in. The monotonic rise of  $M(\chi)$  with  $D$  in the KHAF [Fig. 7(b)] ensures that there is only one crossing point,  $D_c$ , beyond which the finite- $D$  kagome result lies above the  $D = 0$  Husimi one. By establishing the smallest interval in which the  $D = 0$  Husimi curve lies between two kagome curves, as shown in Fig. 8(b), we estimate the error bar on this crossing point and hence conclude that  $D_c = 0.012(2)J$ . We stress that both this value and its error are valid within the confines of the comparison of the kagome to the Husimi lattice, for which no rigorous theoretical justification ex-

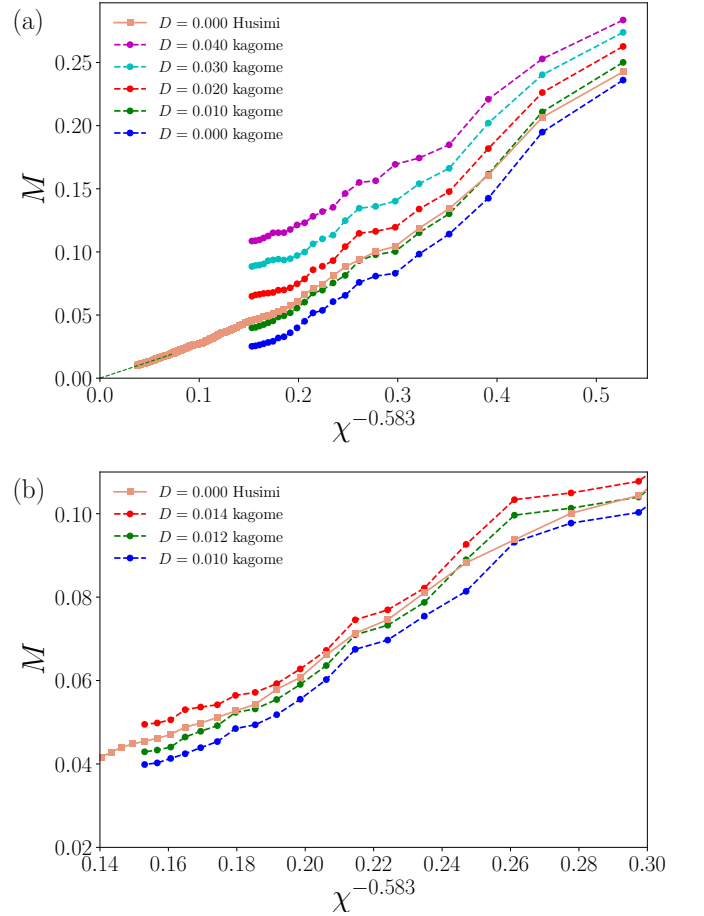


FIG. 8. Staggered magnetization of the KHAF compared with the Husimi HAF. (a)  $M(\chi)$ , shown as a function of  $1/\chi^{0.583}$ , calculated for the Husimi lattice with  $D = 0$  and for the kagome lattice with several values of  $D$ . (b) Detail of  $M(\chi)$  allowing the upper limit of the gapless spin-liquid phase to be established.

ists.

The key qualitative conclusion of our study is that the gapless spin-liquid phase is stable against a finite out-of-plane DM interaction. The persistence of the spin-liquid regime, despite the apparent tendency of the DM term to drive a  $120^\circ$  antiferromagnetically ordered phase, is evidence both for a real physical mechanism underlying the stability of the gapless state and for a certain degree of “protection” against perturbations. We comment in more detail on this issue in Sec. VI. Numerically, the value of  $D_c$  we find is small compared with values in the literature. While one may worry that TNS methods could underestimate this phase boundary by favoring magnetically ordered states in the kagome problem, we caution that our calculation is really not the same problem as that addressed by ED [35, 36] and Schwinger-boson methods [39, 40], because the ground state of the  $D = 0$  spin liquid is quite different. By contrast, the FRG results of Ref. [44] for the KHAF without DM in-

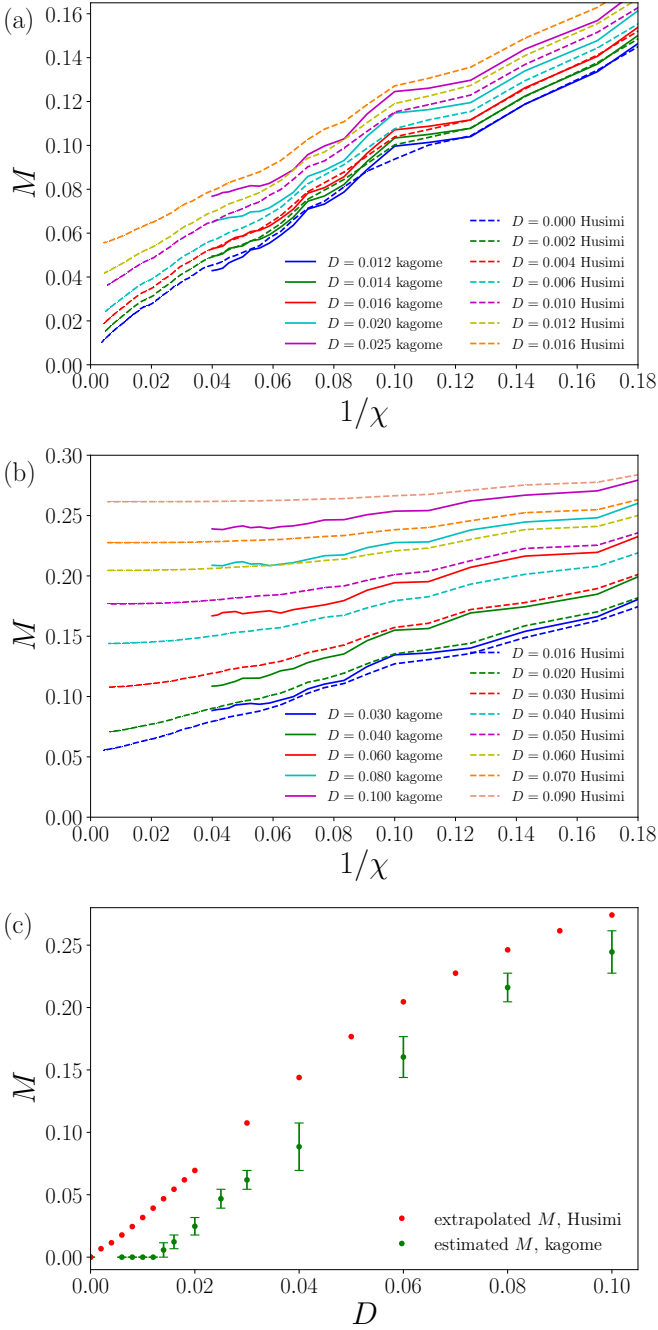


FIG. 9. Staggered magnetization of the KHAF as a function of  $D$ . (a)  $M(\chi)$  for small  $D$  values, where the Husimi results can be used to extract  $M(D)$ . (b)  $M(\chi)$  for larger  $D$  values, where the Husimi results no longer provide an accurate constraint. (c)  $M(D)$  for the kagome lattice compared with the Husimi HAF result of Fig. 6.

interactions are similar or identical to ours, and in this case some uncertainty may reside in the method used to estimate  $D_c$  within the same formalism [43]. A comparison with variational Monte Carlo results would be helpful in this regard. We reiterate the essential point, also made in Ref. [42] that our value of  $D_c$  is finite, even when the

system has a gapless ground state at  $D = 0$ .

We conclude the analysis of our data by extracting  $M$  as a function of  $D$  for the KHAF. Using again the Husimi system as a benchmark, we attempt to find two  $M(\chi)$  curves for the Husimi HAF at different  $D$  values which completely bracket one  $M(\chi)$  curve for the KHAF at fixed  $D$ . We then use the extrapolated  $M$  values of the two Husimi results as the upper and lower bounds for  $M(D)$  on the kagome lattice. This process works rather well at small  $D$ , where the shapes of the  $M(\chi)$  curves are quite similar [Fig. 9(a)], but deteriorates at larger  $D$ , where  $M(\chi)$  for the KHAF dips more strongly at large  $\chi$  [Fig. 9(b)]. Our best estimate for  $M(D)$  is shown in Fig. 9(c), where the growing error bars at higher  $D$  reflect the kagome-Husimi mismatch. It is clear nevertheless that  $M$  on the KHAF remains below the Husimi result, tracking it approximately after the initial offset. Thus the frustrating effects of the additional, longer paths on the kagome lattice appear to be constant, and  $D_z$  does not act, over the range of our study, to create a regime controlled only by the physics of the triangular motifs.

## VI. DISCUSSION

Concerning the physics of the gapless spin liquid, the U(1) Dirac-fermion state is the first [12] and still the leading [14, 15, 17–19] candidate gapless spin-liquid wave function. Simply from the observation that this state is the true ground state, it is tempting to suggest [18] that the mechanism for its stability is to maximize the kinetic energy of mobile spinons. An alternative scenario for the mechanism is to consider maximizing the contributions from gauge fluctuations [68]. However, it has also been suggested, on the basis of ED studies of clusters up to 36 sites [69], that the kagome point in the phase diagram with finite  $J_2$  is a change of phase between two different types of spin liquid, which could explain the appearance of an anomalously low energy scale in the physics of the KHAF. It remains unclear whether such a scenario would indicate a real transition between  $Z_2$  phases or the presence of a U(1) parent phase [17]. The U(1) Dirac state is known to have long-ranged entanglement and a power-law decay of all correlation functions [13].

Our results demonstrate that the U(1) state is not immediately disrupted by out-of-plane DM interactions, i.e. these are not strongly relevant from the point of view of destabilizing the gapless spin liquid. To the extent that the AF-ordered phase is a state of confined spinons, one may conclude that the  $D_z$  term is not immediately confining. We caution that field-theoretical arguments advanced in Ref. [13] do suggest that  $D_z$  should have an immediate effect on the U(1) state, and hence a closer analysis of marginally relevant terms is warranted. Because the U(1) Dirac state has no well-characterized topology, it is not clear that it could enjoy any type of topological protection. It is true that the  $D_z$  term does not break the U(1) symmetry of the system, which may provide

some symmetry protection. This is to be contrasted with an in-plane DM interaction, which does break the U(1) symmetry and could be expected to promote a finite spin scalar product,  $\vec{S}_i \cdot (\vec{S}_j \times \vec{S}_k)$ , on each triangle and hence to favor chiral spin-liquid states. Otherwise the U(1) state may enjoy only “energetic protection” due to the energy gain of its mobile spinons.

From an experimental standpoint, our results imply that herbertsmithite, still by far the best-characterized candidate kagome material, should be in a 120°-ordered state for the proposed value  $D_z/J \approx 0.08$  [31]. One possible explanation may be that the ESR result, which by its nature is an upper bound, is an overestimate. Another, noted in Sec. V, is that our TNS method may be biased towards ordered states, and hence the true  $D_c$  is larger than our estimate, but it is unlikely that our result would contain a factor-10 error. Thus a strong possibility remains that herbertsmithite is, after all, magnetically disordered as a consequence of its structural disorder, i.e. this is an extrinsic effect and the system is not an intrinsic quantum spin liquid. Discounting this possibility would seem to require at minimum a deeper understanding of effects arising due to out-of-plane impurities, specifically as regards in-plane polarization and interplane coupling.

In summary, we have used tensor-network calculations by the method of projected entangled simplex states to demonstrate that the  $S = 1/2$  kagome Heisenberg antiferromagnet retains a gapless quantum spin-liquid ground state for small but finite values of an out-of-plane Dzyaloshinskii-Moriya interaction. Our results imply that herbertsmithite should, based on current estimates, lie well within an antiferromagnetically ordered phase and thus call for a reassessment of the experimental data for this material.

## ACKNOWLEDGMENTS

We thank H.-J. Liao, P. Mendels, J. Reuther, T. Xiang, Z.-Y. Xie, and S. Zvyagin for helpful discussions. This work was supported by Ministry of Science and Technology (MOST) of Taiwan under Grants No. 105-2112-M-002-023-MY3 and 104-2112-M-002-022-MY3, and was funded in part by a QuantEmX grant from ICAM and by the Gordon and Betty Moore Foundation through Grant GBMF5305 to Ying-Jer Kao. We are grateful to the Taiwanese National Center for High-Performance Computing for computer time and facilities.

- 
- [1] L. Savary and L. Balents, Rep. Prog. Phys. **80**, 016502 (2017).
  - [2] P. Mendels and A. S. Wills, in *Introduction to Frustrated Magnetism*, eds. C. Lacroix, P. Mendels, and F. Mila (Springer, Heidelberg, 2011).
  - [3] S. Sachdev, Phys. Rev. B **45**, 12377 (1992).
  - [4] H. C. Jiang, Z. Y. Weng, and D. N. Sheng, Phys. Rev. Lett. **101**, 117203 (2008).
  - [5] S. Yan, D. A. Huse, and S. R. White, Science **332**, 1173 (2011).
  - [6] O. Götze, D. J. J. Farnell, R. F. Bishop, P. H. Y. Li, and J. Richter, Phys. Rev. B **84**, 224428 (2011).
  - [7] S. Depenbrock, I. P. McCulloch, and U. Schollwöck, Phys. Rev. Lett. **109**, 067201 (2012).
  - [8] H. C. Jiang, Z. H. Wang, and L. Balents, Nat. Phys. **8**, 902 (2012).
  - [9] S. Nishimoto, N. Shibata, and C. Hotta Nat. Commun. **4**, 2287 (2013).
  - [10] T. Li, unpublished (arXiv:1601.02165).
  - [11] J.-W. Mei, J.-Y. Chen, H. He, and X.-G. Wen, Phys. Rev. B **95**, 235107 (2017).
  - [12] Y. Ran, M. Hermele, P. A. Lee, and X. G. Wen, Phys. Rev. Lett. **98**, 117205 (2007).
  - [13] M. Hermele, Y. Ran, P. A. Lee, and X. G. Wen, Phys. Rev. B **77**, 224413 (2008).
  - [14] Y. Iqbal, F. Becca, S. Sorella, and D. Poilblanc, Phys. Rev. B **87**, 060405 (2013).
  - [15] Y. Iqbal, D. Poilblanc, and F. Becca, Phys. Rev. B **91**, 020402(R) (2015).
  - [16] Y. Iqbal, D. Poilblanc, and F. Becca, unpublished (arXiv:1606.02255).
  - [17] S. Jiang, P. Kim, J.-H. Han, and Y. Ran, unpublished (arXiv:1610.02024).
  - [18] H. J. Liao, Z. Y. Xie, J. Chen, Z. Y. Liu, H. D. Xie, R. Z. Huang, B. Normand, and T. Xiang, Phys. Rev. Lett. **118**, 137202 (2017).
  - [19] Y.-C. He, M. P. Zaletel, M. Oshikawa, and F. Pollmann, Phys. Rev. X **7**, 031020 (2017).
  - [20] M. P. Shores, E. A. Nytko, B. M. Bartlett, and D. G. Nocera, J. Am. Chem. Soc. **127**, 13462 (2005).
  - [21] P. Mendels, F. Bert, M. A. de Vries, A. Olariu, A. Harrison, F. Duc, J.-C. Trombe, J. S. Lord, A. Amato, and C. Baines, Phys. Rev. Lett. **98**, 077204 (2007).
  - [22] J. S. Helton, K. Matan, M. P. Shores, E. A. Nytko, B. M. Bartlett, Y. Yoshida, Y. Takano, A. Suslov, Y. Qiu, J.-H. Chung, D. G. Nocera, and Y. S. Lee, Phys. Rev. Lett. **98**, 107204 (2007).
  - [23] A. Olariu, P. Mendels, F. Bert, F. Duc, J. C. Trombe, M. A. de Vries, and A. Harrison, Phys. Rev. Lett. **100**, 087202 (2008).
  - [24] T.-H. Han, J. S. Helton, S.-Y. Chu, D. G. Nocera, J. A. Rodriguez-Rivera, C. Broholm, and Y. S. Lee, Nature **492**, 406 (2012).
  - [25] T.-H. Han, M. R. Norman, J.-J. Wen, J. A. Rodriguez-Rivera, J. S. Helton, C. Broholm, and Y. S. Lee, Phys. Rev. B **94**, 060409 (2016).
  - [26] M.-X. Fu, T. Imai, T.-H. Han, and Y. S. Lee, Science **350**, 655 (2015).
  - [27] S.-H. Lee, H. Kikuchi, Y. Qiu, B. Lake, Q. Huang, K. Habicht, and K. Kiefer, Nat. Mater. **6**, 853 (2007).
  - [28] F. Bert, S. Nakamae, F. Ladieu, D. L’Hôte, P. Bonville, F. Duc, J.-C. Trombe, and P. Mendels, Phys. Rev. B **76**, 132411 (2007).



- [29] M. A. de Vries, K. V. Kamenev, W. A. Kockelmann, J. Sanchez-Benitez, and A. Harrison, *Phys. Rev. Lett.* **100**, 157205 (2008).
- [30] D. E. Freedman, T. H. Han, A. Prodi, P. Müller, Q.-Z. Huang, Y.-S. Chen, S. M. Webb, Y. S. Lee, T. M. McQueen, and D. G. Nocera, *J. Am. Chem. Soc.* **132**, 16185 (2010).
- [31] A. Zorko, S. Nellutla, J. van Tol, L. C. Brunel, F. Bert, F. Duc, J. C. Trombe, M. A. de Vries, A. Harrison, and P. Mendels, *Phys. Rev. Lett.* **101**, 026405 (2008).
- [32] S. El Shawish, O. Cépas, and S. Miyashita, *Phys. Rev. B* **81**, 224421 (2010).
- [33] M. Rigol and R. R. P. Singh, *Phys. Rev. Lett.* **98**, 207204 (2007).
- [34] M. Rigol and R. R. P. Singh, *Phys. Rev. B* **76**, 184403 (2007).
- [35] O. Cépas, C. M. Fong, P. W. Leung, and C. Lhuillier, *Phys. Rev. B* **78**, 140405 (2008).
- [36] I. Rousochatzakis, S. R. Manmana, A. M. Läuchli, B. Normand, and F. Mila *Phys. Rev. B* **79**, 214415 (2009).
- [37] P. Sindzingre and C. Lhuillier, *Eur. Phys. Lett.* **88**, 27009 (2009).
- [38] A. M. Läuchli, J. Sudan, and R. Moessner, unpublished (arXiv:1611.06990).
- [39] L. Messio, O. Cépas, and C. Lhuillier, *Phys. Rev. B* **81**, 064428 (2010).
- [40] Y. Huh, L. Fritz, and S. Sachdev, *Phys. Rev. B* **81**, 144432 (2010).
- [41] L. Messio, S. Bieri, C. Lhuillier, and B. Bernu, *Phys. Rev. Lett.* **118**, 267201 (2017).
- [42] W. Zhu, S.-S. Gong, and D. N. Sheng, unpublished (arXiv:1804.03333).
- [43] M. Hering and J. Reuther, *Phys. Rev. B* **95**, 054418 (2017).
- [44] M. Hering, J. Sonnenschein, Y. Iqbal, and J. Reuther, unpublished (arXiv:1806.05021).
- [45] A. Zorko, F. Bert, A. Ozarowski, J. van Tol, D. Boldrin, A. S. Wills, and P. Mendels, *Phys. Rev. B* **88**, 144419 (2013).
- [46] H. Niggemann, A. Klümper, and J. Zittartz, *Z. Phys. B* **104**, 103 (1997);
- [47] T. Nishino, Y. Hieida, K. Okunishi, N. Maeshima, Y. Akutsu, and A. Gendiar, *Prog. Theor. Phys.* **105**, 409 (2001).
- [48] F. Verstraete and J. I. Cirac, unpublished (arXiv:cond-mat/0407066).
- [49] H. H. Zhao, Z. Y. Xie, Q. N. Chen, Z. C. Wei, J. W. Cai, and T. Xiang, *Phys. Rev. B* **81**, 174411 (2010).
- [50] R. Orus, *Ann. Phys.* **349**, 117 (2014).
- [51] J. Eisert, M. Cramer, and M. B. Plenio, *Rev. Mod. Phys.* **82**, 277 (2010).
- [52] Z.-Y. Xie, J. Chen, J.-F. Yu, X. Kong, B. Normand, and T. Xiang, *Phys. Rev. X* **4**, 011025 (2014).
- [53] Y.-J. Kao, Y.-D. Hsieh, and P. Chen, *J. Phys.: Conf. Ser.* **640**, 012040 (2015).
- [54] D. P. Arovas, *Phys. Rev. B* **77**, 104404 (2008).
- [55] H. J. Liao, Z. Y. Xie, J. Chen, X. J. Han, H. D. Xie, B. Normand, and T. Xiang, *Phys. Rev. B* **93**, 075154 (2016).
- [56] H. C. Jiang, Z. Y. Weng, and T. Xiang, *Phys. Rev. Lett.* **101**, 090603 (2008).
- [57] G. Vidal, *Phys. Rev. Lett.* **98**, 070201 (2007).
- [58] R. Orús and G. Vidal, *Phys. Rev. B* **78**, 155117 (2008).
- [59] Z. Y. Xie, H. C. Jiang, Q. N. Chen, Z. Y. Weng, and T. Xiang, *Phys. Rev. Lett.* **103**, 160601 (2009).
- [60] T. Nishino and K. Okunishi, *J. Phys. Soc. Jpn.* **65**, 891 (1996).
- [61] R. Orús and G. Vidal, *Phys. Rev. B* **80**, 094403 (2009).
- [62] L. Vanderstraeten, J. Haegeman, P. Corboz, and F. Verstraete, *Phys. Rev. B* **94**, 155123 (2016).
- [63] L. Wang, I. Pizorn, and F. Verstraete, *Phys. Rev. B* **83**, 134421 (2011).
- [64] Y.-K. Huang, P. Chen, and Y.-J. Kao, *Phys. Rev. B* **86**, 235102 (2012).
- [65] P. Corboz, T. M. Rice, and M. Troyer, *Phys. Rev. Lett.* **113**, 046402 (2014).
- [66] Z. Y. Xie, H. J. Liao, R. Z. Huang, H. D. Xie, J. Chen, Z. Y. Liu, and T. Xiang, *Phys. Rev. B* **96**, 045128 (2017).
- [67] B. Pirvu, G. Vidal, F. Verstraete, and L. Tagliacozzo, *Phys. Rev. B* **86**, 075117 (2012).
- [68] Y.-C. He, Y. Fuji, and S. Bhattacharjee, unpublished (arXiv:1512.05381).
- [69] H. J. Changlani, D. Kochkov, K. Kumar, B. K. Clark, and E. Fradkin, *Phys. Rev. Lett.* **120**, 117202 (2018).